Properties of Partially Denatured Whey Protein Products: Formation and Characterisation of Structure

Zhuo Zhang[1], Valeria Arrighi[2], Lydia Campbell[1,3], Julien Lonchamp[1] & Stephen R. Euston[1*]

[1]Department of Food & Beverage Science, School of Life Sciences, Heriot-Watt University, Edinburgh, EH14 4AS

[2]Institute of Chemical Sciences, School of Engineering and Physical Sciences, Heriot-Watt University, Edinburgh, EH14 4AS

[3]Nandi Proteins Limited, Nine, Edinburgh Bioquarter, Lab 13, Edinburgh, EH16 4UX

[*]Corresponding author S.R.Euston@hw.ac.uk

Abstract

Partially denatured whey protein (PDWPC) products have been manufactured using a controlled heating process that allows control of the degree of denaturation of the whey proteins. This is assessed by following the change in free sulphydryl content of the protein as heating progresses. This allows the formation of soluble whey protein aggregates of diverse particle size and morphology. The PDWPC's have been made using different manufacturing conditions (temperature, pH, degree of denaturation) to give aggregated PDWPC powders with a degree of denaturation in the range 45-98% and particle size 3-17 μm. Particle size analysis, scanning electron microscopy and density analysis show that the particles have aggregated structures that range from compact, particulate gel-like to fibrillar phase-separated structures, with intermediate structures formed under some conditions. These structures are consistent with the known gel structures formed in whey protein concentrate gels. The structure of the PDWPC particles differs from that of microparticulated whey proteins. The possibility of using PDWPC's as ingredients tailored to the needs of food manufacturers is discussed.

Keywords: Whey protein concentrate; microparticulated WPC; partially denatured WPC; scanning electron microscopy

Introduction

For several years food manufacturers have been striving to produce reduced or non-fat foods that have the same texture, taste and consumer acceptance as the high fat equivalent. One strategy that has been used to try to achieve this has been to replace fat with so-called fat mimetics or fat replacers (O'Connor & O'Brien, 2011). Various methods have been used to manufacture fat replacers in the food industry, and the available fat replacers are categorised according to their structure as fat-based, carbohydrate-based or protein based. Fat-based replacers have been manufactured based on two principles. Some such as Olestra (Akoh, 1995; Shahidi & Namal Senanayake, 2007) are polyesters of sucrose where 6-8 fatty acids are esterified with sucrose in much the same way as triglycerides are formed from glycerol and fatty acids. The Olestra molecules have much the same textural properties as fat, but are much larger than triglycerides and so are not broken down in the gut, and thus pass through undigested and contribute no calories to the diet. Other fat based replacers such as Salatrim are triglycerides made with a combination of short and long chain fatty acids. The principle of these is that the short-chained fatty acids have a lower energy density, and the long chained ones a lower absorption, which overall gives a product with less calories than normal triglycerides. Carbohydrate-based and protein-based fat replacers have structures much different from triglycerides and function as replacers in a different way (Shahidi & Namal Senanayake, 2007).

Carbohydrate fat-replacers can be based on starch that has been modified by hydrolysis or substitution, insoluble fibre or soluble high molecular weight gums, and function principally through their ability to alter the viscosity and mouth feel of foods (Sandrou & Arvanitoyannis, 2000; Shahidi & Namal Senanayake, 2007). Protein-based fat mimetics are usually partially denatured through heating, and micro-particulated by the application of shear to break up protein aggregates into small deformable protein particles that are believed to mimic the mouth feel and texture of emulsified fat (Gaull, 1991). In addition to this, protein fat mimetics are usually processed so that they have altered water-binding properties which will lead to an enhanced viscosity of their solutions (Sandrou & Arvanitoyannis, 2000; Shahidi & Namal Senanayake, 2007).

There has been extensive empirical testing of fat mimetics by incorporating them into various foods, and determining their effect on textural and organoleptic properties, thus demonstrating their application in a range of products (Shahidi & Namal Senanayake, 2007). Unfortunately, in general reduced fat products are not favoured by consumers because they do not taste the same or have the same texture as full fat products (McEwan & Sharp, 2000; Hamilton, Knox, Hill & Parr, 2000). There have been few studies that have looked at the mechanisms of action of fat replacers/mimetics even though it is recognised that a fundamental understanding will facilitate formulation of more acceptable low-fat products, and direct the rational design of improved fat

mimetics. In this paper we report on the structural properties of partially denatured whey proteins (PDWPC) that have been manufactured using a novel technology to control the aggregation of proteins during heating (Campbell, 2009). In future publications we will report on the rheological properties of the same products.

The PDWPC products differ from microparticulated proteins in that shear is not used. The aggregates in these products have some similarity to cold-gelling and so-called soluble whey protein aggregates that have been studied and reported previously (Alting, De Jongh, Visschers, & Simons, 2002; Alting, Hamer, De Kruif, & Visschers, 2000; Barbut, 1995; Barbut & Foegeding, 1993; McClements & Keogh, 1995; Nicolai, Britten & Schmitt, 2011; Ryan, Zhong & Foegeding, 2013). Importantly, the partial denaturation technology used allows for greater control over the aggregation process leading to the possibility of forming products that have a range of controlled aggregate particle sizes and properties.

The formation of soluble whey protein aggregates and PDWPC is based on the premise that whey proteins such as β-lactoglobulin (β-lg) and α-lactalbumin (α-lac) exist as stable intermediates during heat processing (McSwiney, Singh & Campanella, 1994; Qi, Brown & Farrell, 2001). This offers the potential for novel ingredients with new functional properties if processing conditions are identified by which the intermediates could be ‘trapped’ before they are transformed into insoluble coagulates towards the end of the

denaturation process. Soluble whey protein aggregates and PDWPC's are believed to be comprised of whey proteins in their molten globule state. The molten globule state has been defined as possessing a compact partially folded structure that has a native-like secondary structure but lacks a fixed tertiary structure (Qi, Brown & Farrell, 2001; Quezada, Schulman, Froggatt, Dobson & Redfield, 2004).

Soluble aggregates have been studied extensively (Nicolai, Britten & Schmitt, 2011). Much of this work has looked at equilibrium aggregation where heating takes place until no further change in particle size occurs. This means that processing has to take place at low protein concentration, below the critical gelation concentration so that discrete aggregates are formed not a continuous gelled network. Recently, Ryan et al. (Ryan, Zhong & Foegeding, 2013) have discussed how soluble aggregate structure might be controlled to produce aggregates of targeted functional properties. However, to date we are not aware of protein products made using these ideas.

In this study part of the PDWPC manufacturing process involves monitoring the percentage denaturation of the protein by measuring the free and total SH-groups in the aggregates and this is used to define heating regimes that can be used to produce products with a controlled degree of denaturation. More details of the process are given in the methods section and in the patent by Campbell (2009). This method allows for a much greater control over the structure and properties of the aggregates and, importantly for manufacturers,

the method allows PDWPC formation at higher protein solids content. The latter is possible because the heating is taken to a controlled degree of denaturation under non-equilibrium conditions rather than to completion of aggregation (equilibrium). This also has the added advantage of shorter heating times.

The aim of this study is to understand better how the structure and morphology of the PDWPCs can be controlled. Through characterization of the PDWPCs we will be able to understand better the origin of the differing rheological properties of the protein aggregates which will be reported in subsequent papers. Characterisation of the PDWPC aggregates will be through determination of macroscopic properties, such as particle size distribution and structures of protein aggregates using electron microscopy as well as the partial specific volumes of the aggregates in solution. Ultimately, this information will be used to tailor aggregate structure and interactions so that controlled rheological properties can be imparted on the PDWPC products.

Material and methods

Partially Denatured Whey Protein Concentrates

Four partially denatured whey protein concentrate (PDWPC) products, a microparticulated whey protein concentrate (MPWPC) and a native whey protein concentrate (WPC) were used in this study. The WPC, Lacprodan87 was a gift from Arla Foods Ingredients, Denmark. Simplesse® 100[E] was a gift

146 from CP Kelco UK Ltd, UK. The PDWPC products were provided by Nandi
147 Proteins Ltd., UK. The PDWPC products were manufactured using a process
148 developed by Nandi Proteins Ltd., some details of which will be given below.
149 Further details can be found in the Nandi Proteins patent for the process
150 (Campbell, 2009). The protein contents of all samples were determined by
151 Kjeldahl nitrogen analysis (Lynch, Barbano & Fleming, 1998) to be 87% for
152 Lacprodan 87, 53% for Simplesse and 60% for PDWPCs.
153 Nandi Protein Ltd has patented a technology that allows control of the solubility,
154 particle size and hence, functionality of protein products through monitoring of
155 the free sulphydryl content of the proteins during the partial denaturation
156 process. The premise is that the free sulphydryl content can be used as a
157 measure of degree of denaturation. To establish processing conditions for
158 PDWPC products, graphs of free sulphydryl content versus temperature under
159 differing conditions of total solids, protein concentration, and pH have been
160 established using the following procedure. Five hundred mL of a whey protein
161 solution of defined total solids, protein content and pH was heated in a water
162 bath at constant temperature whilst stirring. Two mL samples were taken at 1
163 minute intervals and the samples cooled immediately on ice. The free
164 sulphydryl content was determined using the method proposed by Shimada
165 and Cheftel (1989). Three hundred µL of the heated protein sample was added
166 to 10 mL of “sulphydryl buffer” having the following composition 0.086M Tris,
167 4mM EDTA, 0.09M Glycine, 3 mm DTNB (5, 5’-dithiobis(2-nitrobenzoic acid),

168 pH 8. To determine the total SH-groups, 300 µL of each heat treated sample
169 was added to SH-buffer containing 6M urea and 0.5% SDS. The SDS and urea
170 further denatures the protein by dissociating non-covalent hydrophobic bonds
171 causing intra- and intermolecular protein interactions. A series of standard
172 graphs can be defined by plotting free –SH against either time, or against
173 temperature for a defined set of processing conditions (pH, total solids, protein
174 content) which can be used to predict the processing conditions required to
175 process a PDWPC to a given degree of denaturation. Figure 1 shows a typical
176 curve of –SH groups against holding temperature obtained at pH 7.0, 22% total
177 solids where the protein was held at the temperature until an equilibrium
178 proportion of free –SH was achieved. As can be seen in the Figure 1, the
179 percentage of free SH groups increases from 63 to 80ºC, but above 80ºC there
180 is a marked decrease in free -SH groups. Under these experimental conditions,
181 the maximum unfolding of free SH -groups occurs between 78-80 °C. This
182 maximum in free –SH corresponds closely to the denaturation temperature of
183 the major whey protein β-lactoglobulin (de Wit & Swinkels, 1980). At higher
184 temperatures the free SH groups form intra molecular disulphide bonds. The
185 total SH groups remain constant over the temperature range used. The value
186 of free –SH at 20 ºC represent the SH groups that are not disulphide bonded
187 and is taken as being equivalent to 0% denaturation. The rest of the SH groups
188 are in the form of S-S bonds that break during heating but do not reform, and
189 so the free SH content increases. At higher temperatures there is more S-S

190 breakage and a higher free SH content. At a high enough temperature,
191 intra-molecular S-S bonds begin to form and the free –SH content starts to
192 drop. We define the percent denaturation as being the change in free SH
193 between 20 ^{o}C (SH_{20}) and the heating temperature under study (SH_T) divided
194 by the difference between total SH (SH_{Total}) and SH_{20}, i.e.
195
196 $$\frac{SH_T - SH_{20}}{SH_{Total} - SH_T} \qquad (1)$$
197
198 This is only relevant for temperatures below the maximum in free SH. Above
199 this the formation of intermolecular S-S reduces the solubility of the protein
200 aggregates and they become less functional. From Figure 1, the percentage
201 denaturation at 80°C is calculated as 62%. It has been observed that the
202 maximum % denaturation obtained depends on the protein concentration and
203 pH of the heat- treated solution. Protein concentrations less than 10% at pH
204 above 7 are able to reach 100% denaturation, whereas at lower pH the
205 denaturation degree decreases as the pH approaches the iso-electric point. In
206 addition to the temperature of heating, the protein content and the pH are
207 important parameters that can be varied to change the degree of denaturation.
208 Below the peak in –SH, soluble protein aggregates can be made that have
209 interesting and diversified functional properties. If the proteins are processed
210 to a free –SH state above the maximum, however, the proteins form
211 aggregates of reduced solubility and start to lose their functional properties. By

212 controlling the free –SH content during processing the degree of aggregation
213 and functional properties of the proteins can be controlled.
214 The technology outlined above has been used to manufacture four PDWPCs
215 of varied degree of aggregation and hence aggregate particle size for use in
216 this study. Some of the technical details (heating temperature, pH and degree
217 of denaturation) of the manufacturing process are shown are given in Table 1.
218 Each PDWPC samples was prepared from a fresh, cheese whey stream. The
219 whey stream was ultrafiltered to 14% total solids, heat treated to partially
220 denature, cooled to 30 ^{o}C, concentrated to 22-26% TS in a low heat
221 evaporator and spray dried immediately. During heating the free –SH group
222 content is monitored and used as a parameter to control the degree of
223 denaturation achieved. The PDWPC samples have been coded PDWPC's A-D.
224 PDWPC-A is a commercial product, whilst PDWPC's B-D were made on a pilot
225 scale.
226
227 **Particle size distribution**
228 Solutions of WPC, MPWPC and the four PDWPCs were made up at 16%
229 protein content (w/w) in Milli-Q water. The particle size distribution (PSD) of the
230 samples were characterised with either a Mastersizer 2000 (Malvern
231 Instruments Ltd, UK) or a Zetasizer Nano-ZS (Malvern Instruments Ltd, UK),
232 depending on the relative size of the particles. Small aggregate products
233 (WPC, MPWPC) required the Zetasizer, whilst PDWPC particle sizes were

measured using the Masterisizer. Both instruments require an estimate of the refractive index of the particles for calculation of the PSD. Since these are an unknown parameter for the proteins aggregates, we used a method suggested by Hayakawa et al. (1995) and Saveyn et al. (2002) to optimize the refractive index. The particle size distribution was measured using a refractive index of 1.45 for the particle. The data at a refractive index of 1.45 was then recalculated using protein particle refractive indices ranging from 1.35 to 1.80 with an interval of 0.05 (Hayakawa, Nakahira, & Tsubaki, 1995; Saveyn, Mermuys, Thas, & van der Meeren, 2002). The resulting D[0.5] from these calculations was plotted against the refractive index and this graph used to define the optimum refractive index for particles of each of the protein samples. More details of this are given in the results section.

Scanning Electron Microscopy (SEM)

A scanning electron microscope (Model Quanta 650 FEG) (FEI, USA) was used to visualize the structure of particle aggregates in the protein products. Two drops of each protein solution with a concentration of 0.01% (w/w) were spread onto a carbon based, electrically conductive, double sided adhesive disc (known as a Leit tab, Agar Scientific, UK) attached to an SEM aluminium specimen stub (12.5mm diameter, 8mm pin diameter with no grove). Samples were left to dry at room temperature in a dessicator for 2 days and were imaged by SEM at an accelerating voltage of 2kV under high vacuum. Before sample imaging was done, each sample was carbon coated for approximately

5 mins.

Density measurements

The density of different concentrations of each protein sample, and Milli-Q water as a control, were measured with a PAAR DMA 46 density meter (Anton Paar, UK). Protein concentrations, w_p, of 0.4%, 0.8%, 1.2%, 1.5%, 2.3%, 3.0%, 4.6%, 6.0%, 9.0%, 12.0%, and 14.0% (w/w) were made up in Milli-Q water. In this instrument, a U-tube containing the sample is oscillated by an ultrasonic source (Kayukawa, Hasumoto, & Watanabe, 2003). The resonant frequency of the oscillation of the U-tube is dependent on the total mass of the system. The sample mass can be calculated from the resonant frequency, and then the density calculated if the volume of the U-tube is known. From the density results of the serial dilutions of the samples, the partial specific volume of each sample particle in water can be calculated using the mathematical procedure below.

The change in volume of the solution resulting from a unit change in the solute mass is expressed as apparent specific volume of the protein, $\bar{v}$ (Moore, 1976), and defined as

$$\bar{v} = \frac{v - v_0}{c v} \qquad (2)$$

where v and v_0 are the volumes of the solution and the solvent (before the solute is added) and c is the concentration of the solute, or protein, in the solution. With the solution and the solvent densities, ρ and ρ_0, the value of $\bar{v}$

can be calculated as

$$\bar{v} = \frac{1-[(\rho - c)/\rho_0]}{c} \qquad (3)$$

where the expression $(\rho\text{-}c)/\rho_0$ is known as the apparent volume fraction of the solvent, and often denoted as Φ_0 (Galema & Hoiland, 1991; Sarvazyan, 1991). The partial specific volume of the protein molecule in the solution, $\bar{v}^o$, which expresses the properties of the ideal isolated protein molecule, where there are no intermolecular interactions, is obtained by extrapolating $\bar{v}$ to the limit of zero protein concentration (Gekko & Noguchi, 1974; Zhang & Scanlon, 2011).

$$\bar{v}^0 = \lim_{c \to 0} \bar{v} = \lim_{c \to 0} \left(\frac{1-\Phi_0}{c} \right) \qquad (4)$$

The densities, ρ_0 and ρ, were measured with a PAAR DMA 46 density meter (Anton Paar, UK) for water and serial dilutions of each protein. The concentration, c, used for determining the partial specific volumes of the particles are calculated in terms of the total solids in the solution as

$$c = \frac{w_p \rho}{p} \qquad (5)$$

where p represents the protein content of the samples, i.e. 87% for WPC, 53% for MPWPC, and 60% for PDWPC products, respectively.

Results

The refractive index of the particle is required for the calculation of particle size distribution of the protein samples through Mie theory (Du, 2004; Wriedt, 2012).

There have been several studies focusing on the refractive indices of whey proteins, which reported values of refractive indices of 1.615 for α-lactoglobulin, 1.594 for β-lactoglobulin, and 1.606 for bovine serum albumin (McMeekin, Groves, & Hipp, 1964). However, none of these reported values is considered to be accurate for the particle size measurement of the protein and fat replacer materials used here. First of all, the samples in this work are mixtures and thus, are more complicated than pure protein powders. Additionally, the optimized refractive indices, and therefore the particle size distributions, also depend on the equipment employed (Hayakawa et al., 1995). As a result, optimization of the refractive index was performed to ensure that the correct values were used to derive particle size data. Optimization of refractive indices for WPC, MPWPC and PDWPC samples was performed following the method proposed by Hayakawa et al. (1995). The median diameter, D[0.5], of different samples are plotted against refractive indices in Figure 2. It is found that values of D[0.5] for all the samples increase with refractive indices up to a certain refractive index value and then remain constant or decrease. This observation agrees with the results of Hayakawa et al. (1995) and Saveyn et al. (2002). According to these authors, the refractive index corresponding to the first peak of the particle size is considered to be the optimum for calculating the particle size distribution. The optimized refractive index for each sample as deduced from Figure 2 is listed in Table 2.

Particle size distributions of WPC, MPWPC and PDWPC products are

calculated with the optimized refractive indices as listed in Table 2, and the results are illustrated in Figures 3 and 4, respectively. It is found that WPC particles dispersed in water are submicron in size with two peaks in the particle size distribution seen around 0.1 - 0.2 μm and 0.6 - 0.7 μm, respectively. The peak at smaller sizes has been attributed to small soluble aggregates in solutions formed from the proteins (mainly β-lactoglobulin) (Ryan, Zhong, & Foegeding, 2013), while the larger particles are formed by aggregation of the proteins during the processing of the WPC (de la Fuente, Hemar, Tamehana, Munro, & Singh, 2002). For MPWPC, three peaks in the particle size distribution are observed, found around 0.2 μm, 0.9-1.0 μm and 5-6 μm, respectively. The peak corresponding to the smallest particles corresponds to the soluble aggregates formed by the proteins in WPC. The largest of the three peaks (0.9-1.0 μm) corresponds to the particle size of the functional components in MPWPC. The peak around 5-6 μm most likely occurs due to flocculation or aggregation of the smaller particles.

The PDWPC products (Figure 4) are all found to contain micron sized particles when dispersed in water although the shape of the distribution and mean diameters of the particles varies from sample to sample depending on the processing treatment applied. It is observed that PDWPC-A has a wider distribution of particles and a larger mean size than PDWPC-B. Both PDWPC-C and PDWPC-D are found to have similar diameters and particle size distributions in water, as illustrated in Table 2 and Figure 4, and both have

larger average particle sizes than PDWPC-A and PDWPC-B. In general these particle sizes are larger than those for soluble β-lactolgobulin aggregates at pH 6-7, which have been reported by various researchers to be in the range 15-60 nm (Nicolai, Britten & Schmitt, 2011).

In order to understand the aggregates of the proteins in the samples, especially in PDWPC's, scanning electron microscopy (SEM) was employed to image the materials. The electron micrographs of different samples are shown in Figures 5-10. It is found that proteins in WPC are so small as to be barely visible under high magnification (20000x, Figure 5), supporting the small sizes of the particles seen in the particle size distribution for WPC (Figure 3). MPWPC is observed to contain globule-like micron sized particles (Figure 6a). At high magnification (60000x, Figure 6b) the surface of the MPWPC particles does not appear to be smooth, but is irregular suggesting they are formed through aggregation of smaller particles. The MPWPC micrograph (Figure 6a) also contains larger flocs of the smaller particles which would account for the second peak observed in the particle size distribution (Figure 3). PDWPC-A (Figure 7) exhibits particles that are larger than those in MPWPC particles but also appear to be formed from agglomeration of smaller aggregates. These PDWPC-A particles have some similarity to the MPWPC particles, but have more extensive aggregation and larger particles. These large particles observed in PDWPC-A have a dense, compact structure reminiscent of a cauliflower, and their form suggests they may have a self-similar fractal-like

structure. These types of structures are formed via a cluster-cluster type aggregation mechanism (Meakin, 1983; Kolb, Botet & Jullien, 1983). Aggregates of PDWPC-B (Figure 8) are very different in structure to those of MPWPC and PDWPC-A. Aggregates formed in PDWPC-B have a much more open form (Figure 8a) and lack the compact cauliflower-like structure seen in PDWPC-A (Figure 7). At higher magnification (Figure 8b), the particle surface is seen to be made up of short tubule-like protuberances.

Despite similar particle size distributions, the large particles in PDWPC-C and PDWPC-D are found to have very different structures. The micrograph for PDWPC-C (Figure 9) appears to show a large number of very small aggregates filling the field of view, but no obvious large particles. It is possible that this is because any large particles have disintegrated during the dissolution and drying process in preparation for SEM. However, it is clear that any aggregate formed has a differing structure from the other PDWPC's and MPWPC. The particles in PDWP-D (Figure 10) also have a different structure compared to the other protein samples. Here, the particles are formed from large tubule-like structures joined together to form what appears to be an open, porous particle. The tubules are similar to the elongated structures seen on the surface of PDWPC-B particles (Figure 8), but are larger in PDWPC-D (Figure 10), and the particles appear more open with larger pores. At higher magnification, the tubules in PDWPC-D are smooth and lack surface features, unlike the aggregates in PDWPC-A (Figure 8).

It should be noted that it is unadvisable to relate the particle size results in Figures 3 and 4 with the images obtained from SEM, since the former are determined in water solutions while the latter is photographed in vacuum. It should also be remembered that the particle size data is averaged over a large number of particles whilst the SEM images are, necessarily, chosen from a much smaller set of aggregated structures and may not be truly representative of the particle sizes in the sample.

The range of particle structures observed in the PDWPC samples has some similarities to the types of gel structure that can be formed from β-lactoglobulin solutions by changing the pH and ionic strength (Donald, 2008). The gelling properties of WPC and β-lactoglobulin, the major protein in WPC are complex. Two general types of gel structure can be formed, particulate or fine stranded depending on the pH and ionic strength (Clark, Kavanagh & Ross-Murphy, 2001). A third intermediate form, termed a mixed gel which contains both particulate and fine-stranded character is also observed under some conditions (Foegeding, Bowland & Hardin, 1995). At pH close to the isoelectric point (~ 5) and high ionic strength and at neutral pH, high ionic strength electrostatic repulsion between the aggregating protein molecules is low and they form densely packed particulate gels. At pH away from the isoelectric point and low ionic strength fine stranded gels are formed that are fibrillar in nature (Stading, Langton & Hermansson, 1992). The particulate gels are believed to contain proteins of relatively low degree of denaturation and to

form mainly through hydrophobic interaction. These are composed of relatively evenly sized primary aggregates, formed through phase separation that join together to form the gel (Gimel, Durand, Nicolai, 1994; Langton, Astrom & Hermannson, 1997; Kavanagh, Clark & Ross-Murphy, 2000; Ikeda & Morris, 2002). Whey proteins can be made to form the different gel structures through relatively small changes in the physicochemical conditions. For example, Bowland & Foegeding, (1995) have shown that at pH 7 whey protein isolate can be made to form a fine stranded, mixed or particulate gel simply by increasing the ionic strength from 25 mMol (fine stranded) to 75 mMol (mixed) and then to 500 mMol (particulate) using Na_2SO4. A similar range of structures have been observed for soluble whey protein aggregates. Schmidt et al. (Schmitt, Bovay, Rouvet, Shojaei-Rami & Kolodziejczyk, 2007) have shown that aggregate structure ranging from compact spherical (pH 6, no salt), thin curved (pH 7, no salt) to fibrillar (pH 7, high salt) can be achieved when heating at 85 ^{o}C. Based on these observations we can propose that the structure of the PDWPC particles can be explained in terms of the known WPC gel and WPI soluble aggregate structures, although the structures formed here will differ due to differences in the conditions used during aggregate formation. PDWPC's A and B have a similar particle size, and are made at similar pH and temperatures. The difference is the degree of denaturation that they have been processed to, 65% for PDWPC-A and 41% for PDWPC-B (Table 1). The higher degree of denaturation for PDWPC-A suggests the protein molecules are more

extensively unfolded, and likely to have a greater exposure of the hydrophobic core of the molecule. Thus, the proteins in PDWPC-A can interact more extensively with each other through hydrophobic interactions compared to PDWPC-B. This would explain both the larger particles size of the PDWPC-A aggregates, and the more densely packed structure compared to PDWPC-B. The relatively low pH will also contribute to the close packed structure.

For PDWPC-C and PDWPC-D the pH is 7.0 and the temperature either the same as for PDWPC's A and B (72.5 ^{o}C for PDWPC-C) or higher (74 ^{o}C for PDWPC). The particle size for both these PDWPC's is much larger (17 μm for both, Table 2). The degree of denaturation, however, differs greatly for the two – 51% for PDWPC-C and 98% for PDWPC-D (Table 1). This suggests that the particle size is not necessarily a factor of the degree of denaturation, but that the processing pH plays a role as well. Explaining the mechanism of formation of PDWPC-C is difficult because we were unable to obtain good SEM micrographs of the structure, presumably because the structure was not strong enough to withstand preparation for microscopy. This may be because the aggregates although large are formed from weakly interacting proteins. The relatively low degree of denaturation and pH further from the isoelectric point than for PDWPC-A and B (i.e. a higher net charge for the proteins) would mean weak hydrophobic interactions coupled with greater electrostatic repulsion will control the interactions in the aggregate, and presumably these are weak. For PDWPC-D the higher degree of denaturation will give rise to

more exposed hydrophobic areas of the proteins, and thus a greater hydrophobic interaction between the proteins. Presumably, it is this greater hydrophobic interaction that leads to the morphology of the PDWPC-D particles (Figure 10). Here, the open, tubular aggregates are typical of a phase-separated system where there are strong interactions that lead to a separation into protein rich and depleted regions. This could also explain the smooth surface of the aggregates in the SEM micrographs for PDWPC-D compared to PDWPC-A and B, since PDWPC-D aggregates are likely to contain very dense regions of protein that are very closely packed together. Interestingly, we have observed a similar tendency to form both phase separated and compact globular aggregates in computer models of protein aggregation in which the degree of unfolding and interaction strength of the model proteins are varied (Costello & Euston, 2006).

The specific density, ρ_{sp}, can be used to express the changes in density of the protein solutions, where,

$$\rho_{sp} = \frac{\rho}{\rho_0} - 1 \qquad (6)$$

where ρ represents the absolute density value (protein plus solvent) and the subscript $_0$ indicates properties of the solvent, here water. The specific density of different concentrations of WPC, MPWPC and PDWPC's are plotted versus total solid concentration in Figure 11. It is found that the specific density, ρ_{sp}, has a good a linear relationship ($R^2 > 0.998$) with the total solid concentration

of the serial dilutions for all protein samples. It should be noted that the intercepts of the regression lines of ρ_{sp} in Figure 11 are set to be 0 according to the definition of specific density. As expected, the density of the solution increases with the addition of protein. The concentration dependence of specific density, $d\rho_{sp}/dw$, which is numerically equal to the slopes, $[\rho_{sp}]$, of the lines in Figure 11, is shown in Tables 3. From Figure 11 and Table 3, it is found that the modified protein product solutions have a higher density than WPC solutions, with the MPWPC and PDWPC's having a similar dependence of density on concentration. This will be due in part to the more densely packed aggregates observed in the aggregated products, but possibly also because they contain a higher proportion of non-protein material which could have a higher density than the protein. The volume fraction, $\varphi=1-\Phi_0$, of the total solids in the serial dilutions are calculated using equation (3) and plotted versus the total solid content in Figure 12. As with the plot of ρ *vs* w, a linear relationship is also observed between φ and *w*, and the φ at a given concentration is higher for WPC than for the other protein products.

The apparent specific volume of solute in the solutions, $\bar{v}$, is calculated from the density and the solute concentration using Equation 2, where the solute concentration, *c* (in mg/ml), is calculated from the density, ρ, and the total solid content, *w* (in %), as c = ρw. Values of the apparent specific volume, $\bar{v}$, of WPC and the protein-based fat replacers are plotted in Figure 13. According to Figure 13, the modified whey proteins are found to have smaller specific

volume than the fat replacers, which is believed to be due to unfolding of the polypeptide chains and loss of the void hydrodynamic core of the protein molecules (Chalikian, 2003). For all protein samples the $\bar{v}$ is independent of concentration at high concentrations. Since the concentration clearly influences the specific volume of proteins due to protein-protein interactions, the partial specific volume at infinite dilution, $\bar{v}^0$, is commonly employed to investigate the molecular structure of isolated proteins (Sarvazyan, 1991). It is observed that the values of $\bar{v}$ for all the samples in Figure 13 increase at low concentrations (< 6%), while the values are approximately constant at high concentrations (> 6%). Pavlovskaya et al. (1992) consider that the region where $\bar{v}$ is increasing (w < 6%) corresponds to dilute solution behaviour (Pavlovskaya, McClements, & Povey, 1992). Extrapolation of the partial specific volume of the protein back to w=0 in the dilute regime (w< 6%) is carried out to enable determination of $\bar{v}^0$ at infinite dilution. Values of $\bar{v}^0$ for WPC and modified proteins are shown in Table 4. This property provides information on the protein structure at the molecular levels (Chalikian, 2001; Chalikian, Totrov, Abagyan, & Breslauer, 1996). It is found the value of $\bar{v}^0$ for WPC (0.723) is close to but slightly smaller than those for pure β-lactoglobulin and bovine serum albumin, which have been reported to range from 0.734 ~ 0.751 cm^3/g by Valdez, Le Huérou, Gindre, Urbach, and Waks (2001) and 0.736 cm^3/g by Bernhardt and Pauly (1975). The values of $\bar{v}^0$ for MPWPC and PDWPC products are smaller than that of WPC.

When the density and specific volume results are taken together they support the observations from the SEM. WPC has the lowest density of the protein solutions, and WPC proteins occupy a larger volume per gram of protein. This is consistent with a hydrated native protein molecular structure that, although folded, is not highly compacted. For the aggregated proteins, the density of solutions and the specific volume suggest a much more compact structure where the protein molecules in the aggregates are much more closely packed, and the particles more dense. The solution density and the specific volumes for the MPWPC and PDWPC's differ little between samples (only by about 5%). However, if the results are looked at closely, some trends can be seen that are consistent with the structures seen in the SEM micrographs. The slopes of the specific density graphs (Figure 11) for MDWPC and PDWPC-A are about 3-5% greater than for PDWPC-B, C and D. This again is consistent with the more compact, particulate gel-like nature of the MPWPC and PDWPC-A particles (Figures 6 and 7) compared to the more open mixed or fibrillar-like structures seen in the PDWPC-B, C and D aggregates (Figures 8-10). The specific volume (Figure 13) and partial specific volume (Table 4) for PDWPC-A is lower than for the other PDWPC's which indicates that the aggregates occupy a smaller volume per unit mass, which again points to a more dense structure. For MPWPC, however, the compact particulate like structure is not reflected in the specific volume and partial specific volume data, which may be a consequence of the smaller size of the aggregates compared to PDWPC-A, or

the tendency of the MPWPC particles to form more open flocs in solution.

Conclusions

We have shown that by controlling the processing conditions it is possible to form aggregated whey protein products that have differing structures, size distributions and solution properties. These particles are believed to be formed from globular whey proteins that are not fully denatured, but are in a molten-globule-like state. Scanning electron microscopy has shown that the structures of the particles are consistent with the known structures of whey protein gels, but are formed on a smaller scale. These range from compact particulate-gel like particles to those with a fibrillar or mixed structure. The aggregates appear to be formed in the same way as previously reported soluble whey protein aggregates, but are formed under conditions which offer greater control of structure and functionality. In subsequent papers it will also be shown that the differing particles structures give rise to differences in the rheological properties of solutions of the protein products. The partial denaturation technology has already been used to make a product that has been marketed commercially. It is expected that with further research a range of partially denatured protein products could be made that have particle aggregate structures and therefore functional properties that are tailored to the requirements of a particular food application.

Acknowledgements

ZZ acknowledges receipt of a PhD Scholarship from the Heriot-Watt University Life Science-Physical Science Interface Theme.

References

Akoh, C.C, (1995). Lipid based fat substitutes. *Critical Reviews in Food Science & Nutrition*, **35**, 405-430.

Alting A.C, Hamer R.J., de Kruif C.G. , Visschers R.W. (2000). Formation of disulfide bonds in acid induced gels of preheated whey protein isolate. *Journal of Agriculture and Food Chemistry*, **48** 5001-5007

Alting, A.C, de Jongh, H.H.J., Visschers, R.W. & Simons (2002). Physical and chemical interactions in cold gelation of food proteins. *Journal of Agriculture and Food Chemistry*, **50**, 4682-4689.

Barbut, S., & Foegeding, E.A. (1993). Ca^{2+}-induced gelation of pre-heated whey protein isolate. *Journal of Food Science*, **58**, 867-871.

Bernhardt, J., & Pauly, H. (1975). Partial specific volumes in highly concentrated protein solutions. I. Water-bovine serum albumin and water-bovine hemoglobin. *The Journal of Physical Chemistry*, **79**, 584–590.

Bowland, E.L. & Foegeding, E.A. (1995). Effects of anions on thermally-induced whey-protein gels. *Food Hydrocolloids*, **9**, 47-56.

Campbell, L.J. (2009). Protein denaturation control. EU Patent: EP2104433.

Chalikian, T.V. (2001). Structural thermodynamics of hydration. *Journal of Chemical Physics*, **105**, 12566-12578.

Chalikian, T.V. (2003). Volumetric properties of proteins. *Annual Review of Biophysics and Biomolecular Structure*, **32**, 207-235.

Chalikian, T.V., Totrov, M., Abagyan, R., & Breslauer, K.J. (1996). The

589 hydration of globular proteins as derived from volume and compressibility
590 measurement: Cross correlating thermodynamic and structural data. *Journal*
591 *of Molecular Biology*, **260**, 588-603.
592 Clark, A.H., Kavanagh, G.M. & Ross-Murphy, S.B. (2000). Globular protein
593 gelation - theory and experiment. *Food Hydrocolloids*, **15**, 383-400.
594 Costello, G. & Euston, S.R. (2006). A Monte Carlo simulation of the
595 denaturation, aggregation phase separation and gelation of model globular
596 molecules. *Journal of Physical Chemistry B*, 110, 10151-10164.
597 de la Fuente, M.A., Hemar, Y., Tamehana, M., Munro, P.A., & Singh, H. (2002).
598 Process-induced changes in whey proteins during the manufacture of whey
599 protein concentrates. *International Dairy Journal*, **12**, 361-369.
600 de Wit, J.N. & Swinkels, G.A. (1980). A differential scanning calorimetric study
601 of the thermal denaturation of bovine beta-lactoglobulin. Thermal behaviour at
602 temperatures up to 100 ^{o}C. *Biochimica et Biophysica Acta*, **624**, 40–50.
603 Donald, A.M. (2008). Aggregation in β-lactoglobulin. *Soft Matter*, **4**, 1147-1150.
604 Du, H. (2004). Mie-scattering calculation. *Applied Optics*, **43**, 1951-1956.
605 Foegeding, E.A., Bowland, E.L. & Hardin, C.C. (1995). Factors that determine
606 the fracture properties and microstructure of globular protein gels. *Food*
607 *Hydrocolloids*, **9**, 237-249.
608 Galema, S.A., & Hoiland, H. (1991). Stereochemical aspects of hydration of
609 carbohydrates in aqueous-solutions. 3. Density and ultrasound measurements.
610 *The Journal of Physical Chemistry*, **95**, 5321-5326.

611 Gaull, G.E. (1991). Role of micro-particulated protein fat substitutes in food and
612 nutrition. *Annals of the New York Academy of Sciences*, **623**, 350-355.
613 Gekko, K., & Noguchi, H. (1974). Hydration behaviour of ionic dextran
614 derivatives. *Macromolecules*, **7**, 224-229.
615 Gimel, J.C., Durand, D. & Nicolai, T. (1994). Structure and distribution of
616 aggregates formed after heat-induced denaturation of globular proteins.
617 *Macromolecules*, **27**, 583-589.
618 Hamilton, J., Knox, B., Hill, D. and Parr H. (2000) Reduced fat
619 products—consumer perceptions and preferences. *British Food Journal*, **102**,
620 494–506.
621 Hayakawa, O., Nakahira, K., & Tsubaki, J.I. (1995). Estimation of the optimum
622 refractive index by the laser diffraction and scattering method-On the raw
623 material of fine ceramics. *Advanced Powder Technology*, **6**, 47-61.
624 Ikeda, S., & Morris, V.J. (2002). Fine-stranded and particulate aggregates of
625 heat-denatured whey proteins visualized by atomic force microscopy.
626 *Biomacromolecules*, **3**, 382-389.
627 Ju, Z.Y. & Kilara, A. (1998). Effects of preheating on properties of aggregates
628 and of cold-set gels of whey protein isolate. *Journal of Agricultural and Food*
629 *Chemistry*, **46**, 3604-3608.
630 Kayukawa, Y., Hasumoto, M., & Watanabe, K. (2003). Rapid density
631 measurement system with vibrating-tube densimeter. *Review of Scientific*
632 *Instruments*, **74**, 4134-4139.

633 Kolb, M., Botet, R. & Jullien, R. (1983). Scaling of kinetically growing clusters.
634 *Physical Review Letters*, **51**, 1123-1126.
635 Langton, M., Astrom, A. & Hermansson, A.M. (1997). Influence of the
636 microstructure on the sensory quality of whey protein gels. *Food Hydrocolloids*,
637 **11**, 217-230.
638 Lynch, J.M., Barbano, D.M. & Fleming, J.R. (1998). Indirect and direct
639 determination of the casein content of milk by Kjeldahl nitrogen analysis:
640 collaborative study. *Journal of AOAC International*, **81**, 763-774.
641 McClements, D.J., & Keogh, M.K. (1995). Physical properties of cold-setting
642 gels formed from heat-denatured whey protein isolate. *Journal of the Science*
643 *of Food and Agriculture*, **69**, 7-14.
644 McEwan, J.A. and Sharp, T.M. (2000) Technical, economic and consumer
645 barriers to the consumption of reduced fat bakery products, *Nutrition & Food*
646 *Science*, **30**, 16–18.
647 McMeekin, T.L., Groves, M.L., & Hipp, N.J. (1964). Refractive indices of amino
648 acids, proteins, and related substances. In J. A. Stekol (Ed.), *Amino Acids and*
649 *Serum Proteins (Vol. 44)*. Washington, DC, USA: American Chemical Society.
650 McSwiney, M., Singh, H. & Campanella O.H. (1994). Thermal aggregation and
651 gelation of bovine beta-lactoglobulin. *Food Hydrocolloids*, **8**, 441–453.
652 Meakin, P. (1983). Formation of fractal clusters and networks by irreversible
653 diffusion-limited aggregation. *Physical Review Letters*, **51**, 1119-1122.
654 Mleko, S. (1999). Effect of protein concentration on whey protein gels obtained

by a two-stage heating process. *European Food Research and Technology*, **209**, 389-392.

Moore, W.J. (1976). Physical Chemistry (5th ed.). London, UK: Longman Group Limited.

Nicolai, T., Britten, M. & Schmitt, C. (2011). β-Lactoglobulin and WPI aggregates: formation, structure and applications. *Food Hydrocolloids*, **25**, 1945–1962.

O'Connor, T.P. & O'Brien, N.M., (2011). Fat Replacers. In Encyclopaedia of Dairy Sciences (2nd Edn), 528-532.

Pavlovskaya, G., McClements, D.J., & Povey, M.J.W. (1992). Ultrasonic investigation of aqueous solutions of globular protein. *Food Hydrocolloids*, **6**, 253-262.

Qi P.I., Brown E. M., Farrell H. M. (2001). New views on structure–function relationships in milk proteins. *Trends in Food Science & Technology*, **12**, 339-346.

Quezada, C.M., Schulman, B.A., Froggatt, J.J., Dobson, C.M., Redfield, C. (2004). Local and global cooperativity in the human alpha lactalbumin molten globule, Journal of Molecular *Biology*, **338**, 149-158

Ryan, K.N., Zhong, Q., & Foegeding, E.A. (2013). Use of whey protein soluble aggregates for thermal stability - A hypothesis paper. *Journal of Food Science*, **78**, R1105-R1115.

Sandrou, D.K., & Arvanitoyannis, I.S. (2000). Low-fat/calorie foods: Current

677 state and perspectives. *Critical Reviews in Food Science and Nutrition*, **40**,
678 427-447.
679 Sarvazyan, A.P. (1991). Ultrasonic velocimetry of biological compounds.
680 *Annual Reviews of Biophysics and Biophysical Chemistry,* **20**, 321-342.
681 Saveyn, H., Mermuys, D., Thas, O., & van der Meeren, P. (2002).
682 Determination of the refractive index of water-dispersible granules for use in
683 laser diffraction experiments. *Particle & Particle Systems Characterization,* **19**,
684 426-432.
685 Schmitt, C., Bovay, C., Rouvet, M., Shojaei-Rami, S. & Kolodziejczyk, E.
686 (2007). Whey protein soluble aggregates from heating with NaCl:
687 physicochemical, interfacial, and foaming properties. *Langmuir*, **23**,
688 4155–4166.
689 Shahidi, F. & Namal Senanayake, S. P. J. (2007). Fat Replacers. In
690 *Kirk-Othmer Encyclopedia of Chemical Technology*, online edition, DOI:
691 10.1002/0471238961.06012013151819.a01.pub2
692 Shimada, K., & Cheftel, J.C. (1989). Sulfhydryl group/disulfide bond
693 interchange reactions during heat-induced gelation of whey protein isolate.
694 *Journal of Agricultural & Food Chemistry,* **37**, 161-168.
695 Stading, M., Langton, M., & Hermansson, A. (1992). Inhomogeneous
696 fine-stranded b-lactoglobulin gels. *Food Hydrocolloids,* **6**, 455-470.
697 Valdez, D., Le Huérou, J.Y. , Gindre, M., Urbach, W., & Waks, M. (2001).
698 Hydration and protein folding in water and in reverse micelles: Compressibility

and volume changes. *Biophysical Journal,* **80**, 2751-2760.

Wriedt, T. (2012). Mie theory: A review. In W. Hergert & T. Wriedt (Eds.), *The Mie Theory Basics and Applications*. New York, USA: Springer-Verlag Berlin Heidelberg, pp. 53-71.

Zhang, Z., & Scanlon, M.G. (2011). Solvent effects on the molecular structures of crude gliadins as revealed by density and ultrasound velocity measurements. *Journal of Cereal Science*, **54**, 181-186.

Table Legends.

Table 1 - Protein contents of samples and process conditions for WPC, MPWPC and PDWPC products.

Table 2 - Optimized refractive indices and the corresponding median diameter, D[0.5] of different samples.

Table 3 - Concentration dependence of specific density, ρ_{sp}, of different proteins products.

Table 4 - Partial specific volume, $\bar{v}^0$, of different protein products.

Figure Legends

Figure 1 - Denaturation of WPC with temperature as indicated by the content of free sulphydryl. This graph was prepared for a solution of cheese whey concentrated to 22% total solids by ultrafiltration, adjusted to pH 7 and heated at various temperatures until no change in the free sulphydryl content was found.

Figure 2 Refractive index dependence of the median diameter, D[0.5], for WPC, MPWPC, PDWPC-A, PDWPC-B, PDWPC-C and PDWPC-D. Data for WPC and MPWPC are measured with a Malvern Zetasizer, and the PDWPC samples with a Malvern Mastersizer.

Figure 3 Particle size distribution of WPC and MPWPC measured with a Malvern Zetasizer.

Figure 4 Particle size distribution of PDWPC products measured with a Malvern Mastersizer.

Figure 5 Scanning electron micrograph of WPC with a magnification of 30000x.

Figure 6 Electron micrograph of MPWPC with a magnification of (a) 4000x and (b) 60000x.

Figure 7 Electron micrograph of PDWPC-A with a magnitude of (a) 16000x and (b) 60000x.

Figure 8 Electron micrograph of PDWPC-B with a magnitude of (a) 3084x and (b)12000x.

738 **Figure 9** Electron micrograph of PDWPC-C with a magnitude of (a) 4000x and
739 (b) 30000x.
740 **Figure 10** Electron micrograph of PDWPC-D with a magnitude of (a) 5000x
741 and (b) 24000x.
742 **Figure 11** Specific density ρ_{sp}, of serial dilutions of WPC, MPWPC, and
743 PDWPC products.
744 **Figure 12** Volumetric fraction, φ, of serial dilutions of WPC, MPWPC and
745 PDWPC products.
746 **Figure 13** Apparent specific volume, $\bar{v}$, of WPC, MPWPC and PDWPC
747 products.
748
749

Table 1

	Protein content (%)	Process conditions		
		Temperature (ºC)	pH	Degree of denaturation (%)
WPC	87	-	-	-
MPWPC	53	-	-	-
PDWPC-A	60	73	6.5	65
PDWPC-B	60	72.5	6.4	45
PDWPC-C	60	72.5	7.0	51
PDWPC-D	60	74	7.0	98

Table 2 -

Sample	Optimized Refractive Index	Median Diameter / D[0.5] (μm)
WPC	1.40	0.48 ± 0.04
MPWPC	1.40	1.72 ± 0.04
PDWPC-A	1.50	5.48 ± 0.001
PDWPC-B	1.55	3.30 ± 0.001
PDWPC-C	1.45	17.00 ± 0.07
PDWPC-D	1.40	17.00 ± 1.00

759

760 **Table 3 -**

	Protein content (%)	$[\rho_{sp}]$	R^2
WPC	87	0.2676	0.9998
MPWPC	53	0.3319	0.9986
PDWPC-A	60	0.3368	0.9990
PDWPC-B	60	0.3194	0.9993
PDWPC-C	60	0.3195	0.9994
PDWPC-D	60	0.3205	0.9993

761

762

763

764 **Table 4 -**

	$\bar{v}^0$ (cm^3/g)
WPC	0.723 ± 0.006
MPWPC	0.685 ± 0.004
PDWPC-A	0.664 ± 0.001
PDWPC-B	0.684 ± 0.007
PDWPC-C	0.680 ± 0.006
PDWPC-D	0.680 ± 0.002

765

766

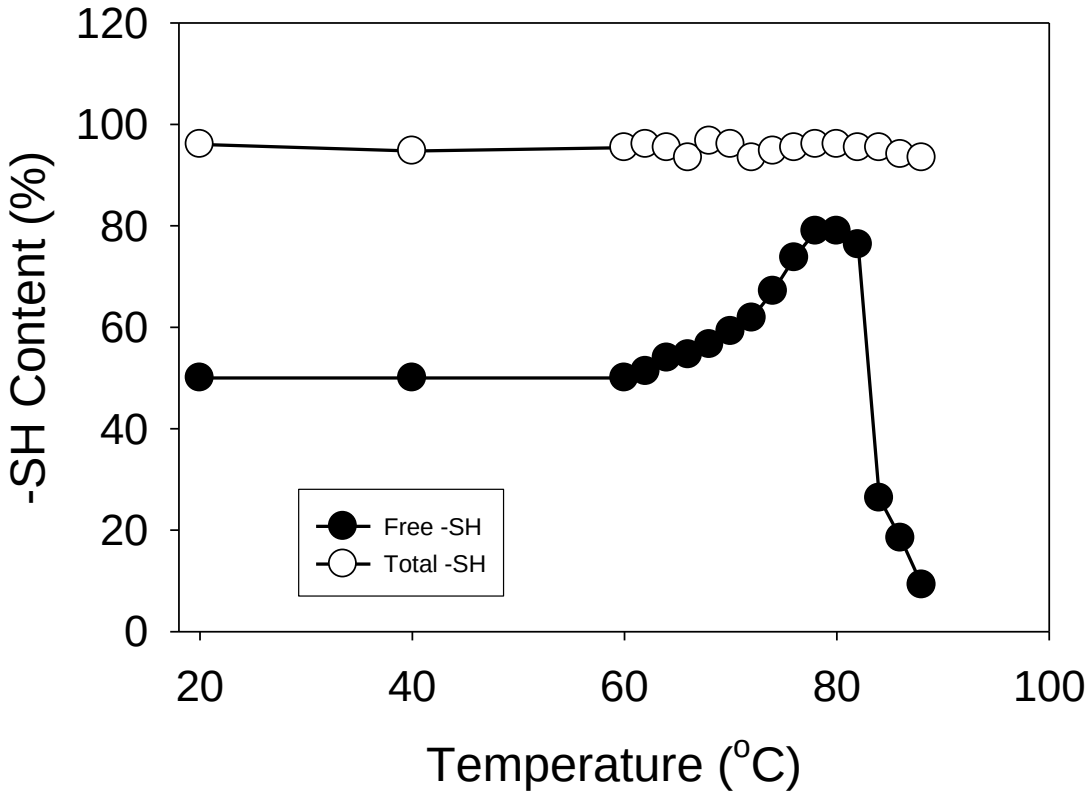

767

768

769 **Figure 1**

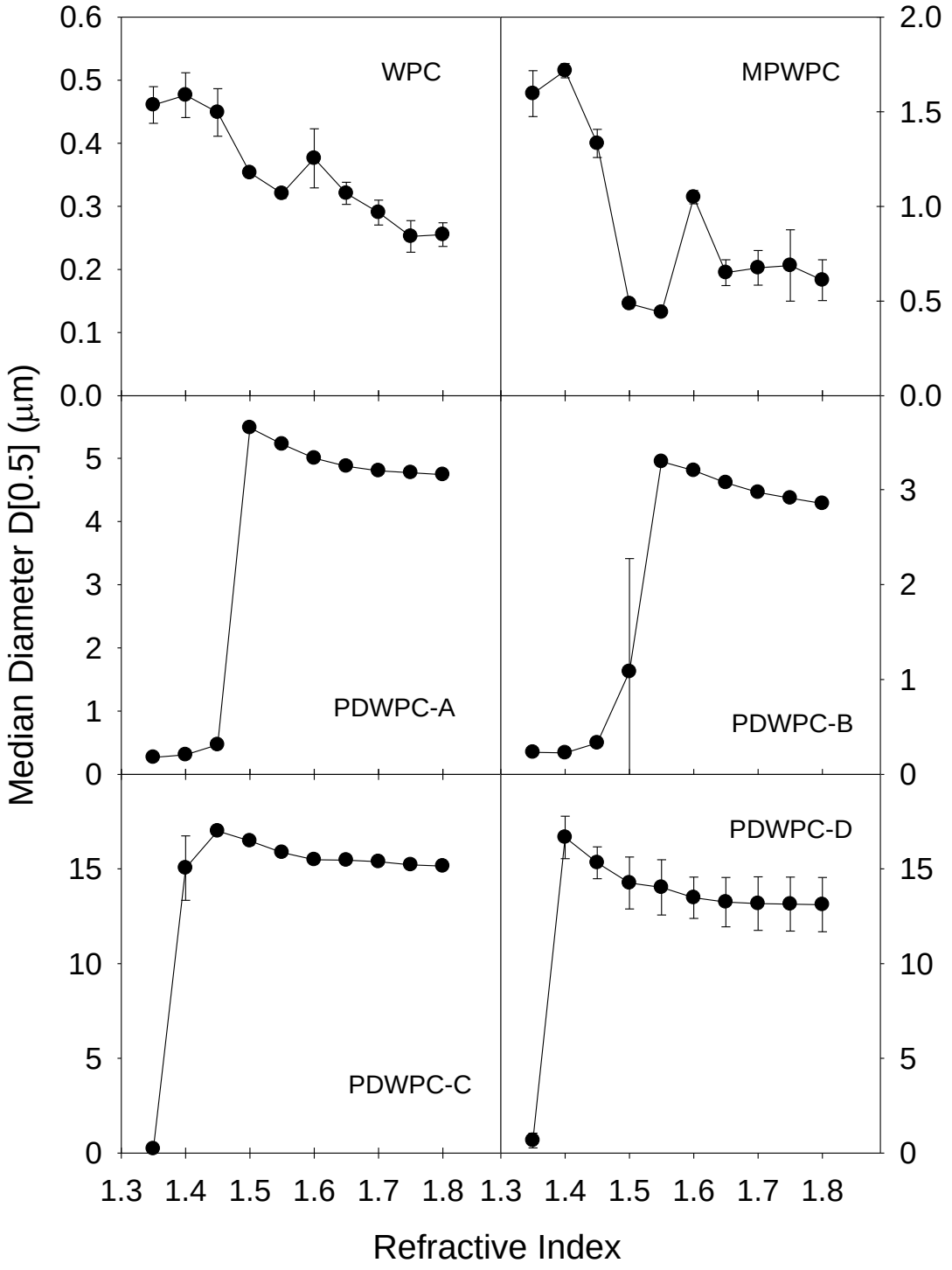

770

771 **Figure 2**.

772

773

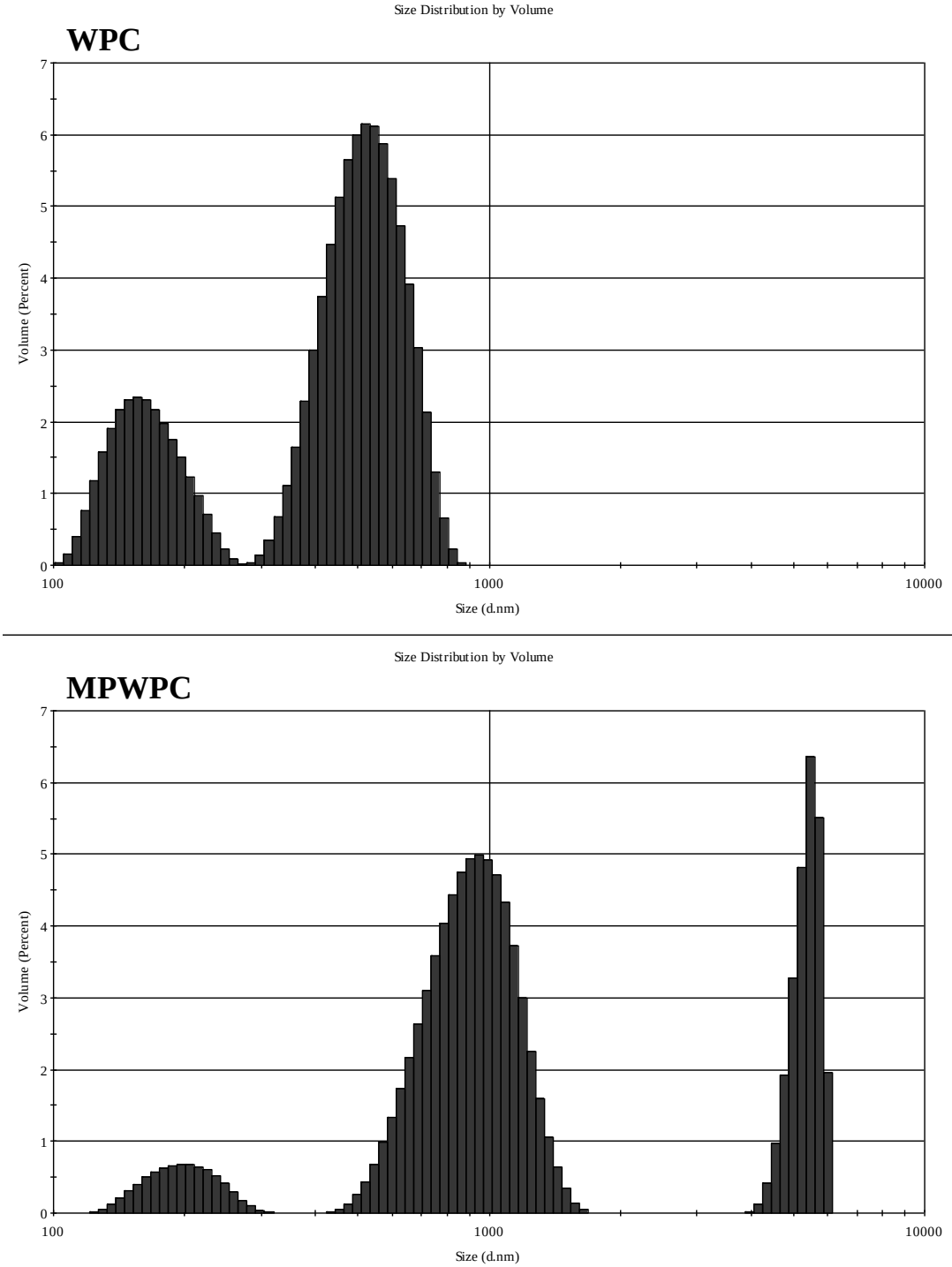

774

775 **Figure 3**

776

777

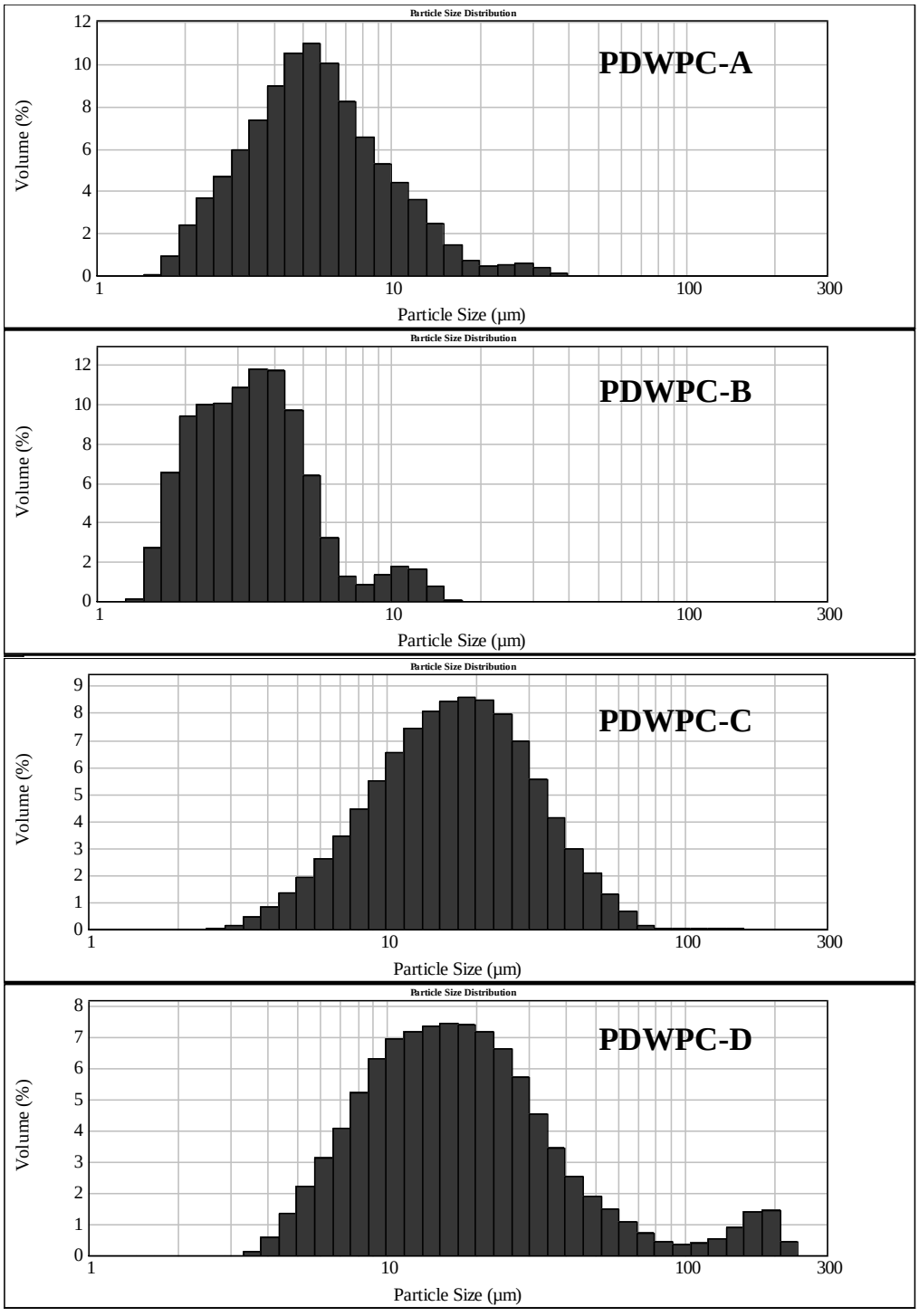

778

779 **Figure 4**

780

781 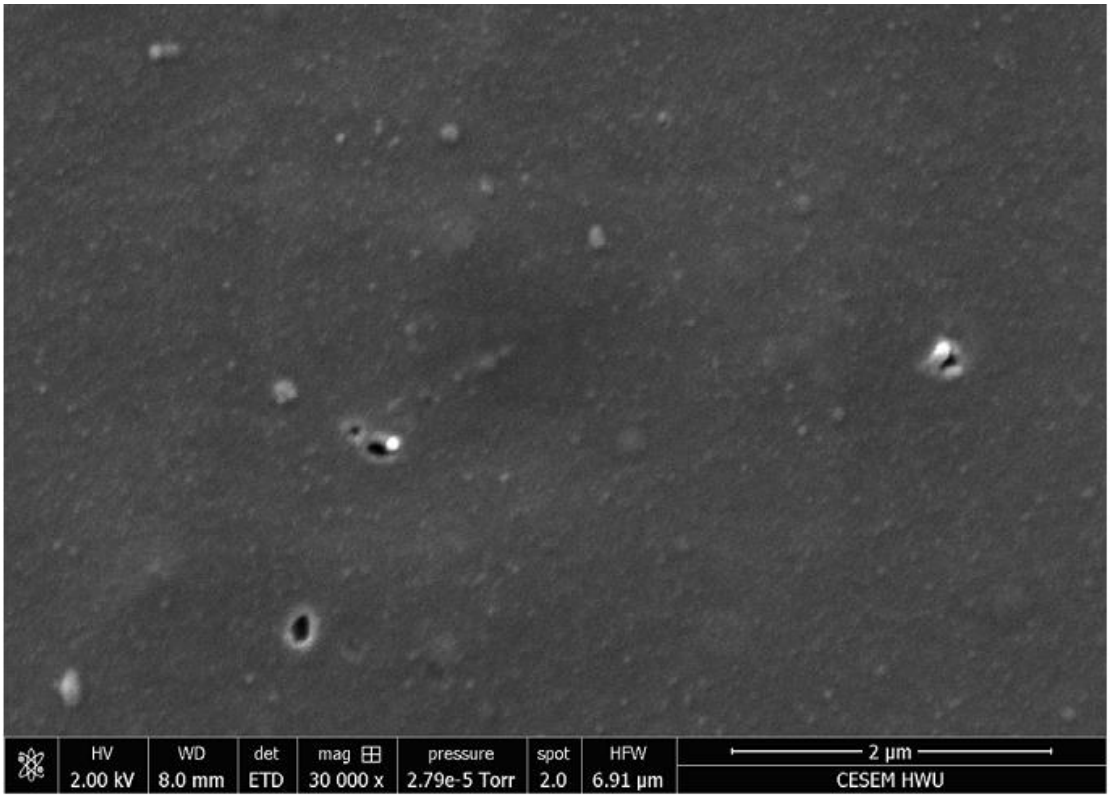

782

783 **Figure 5**

784

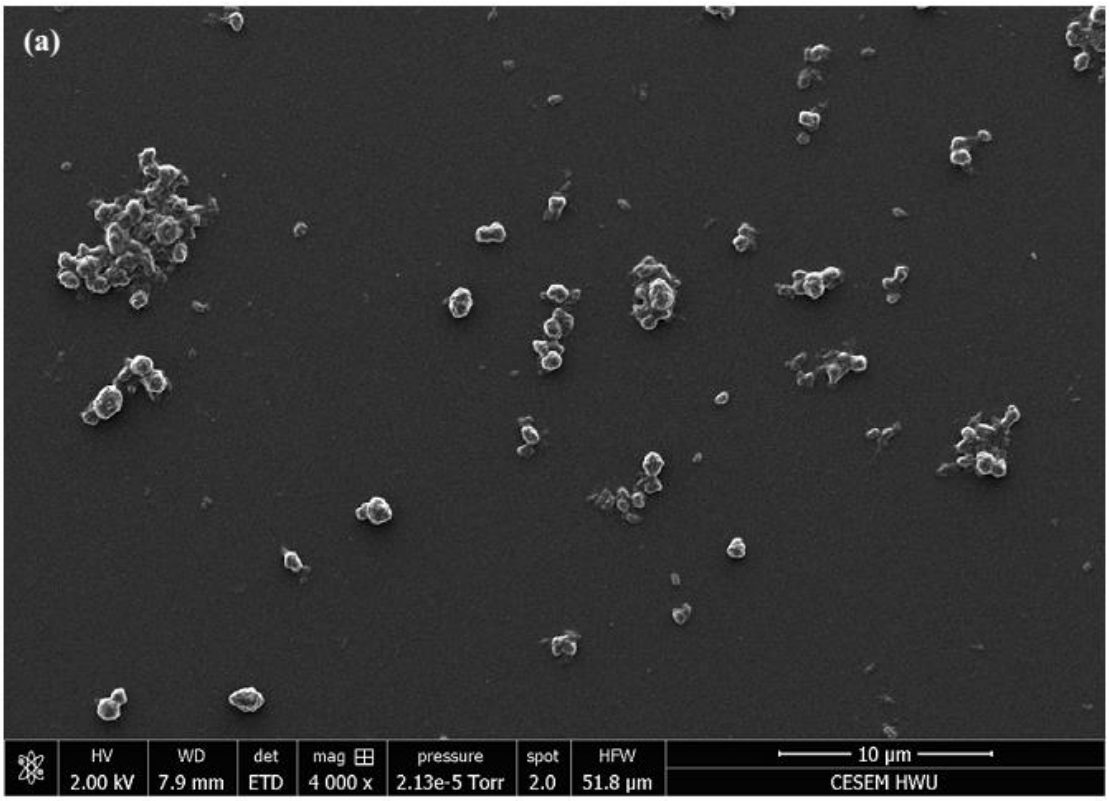

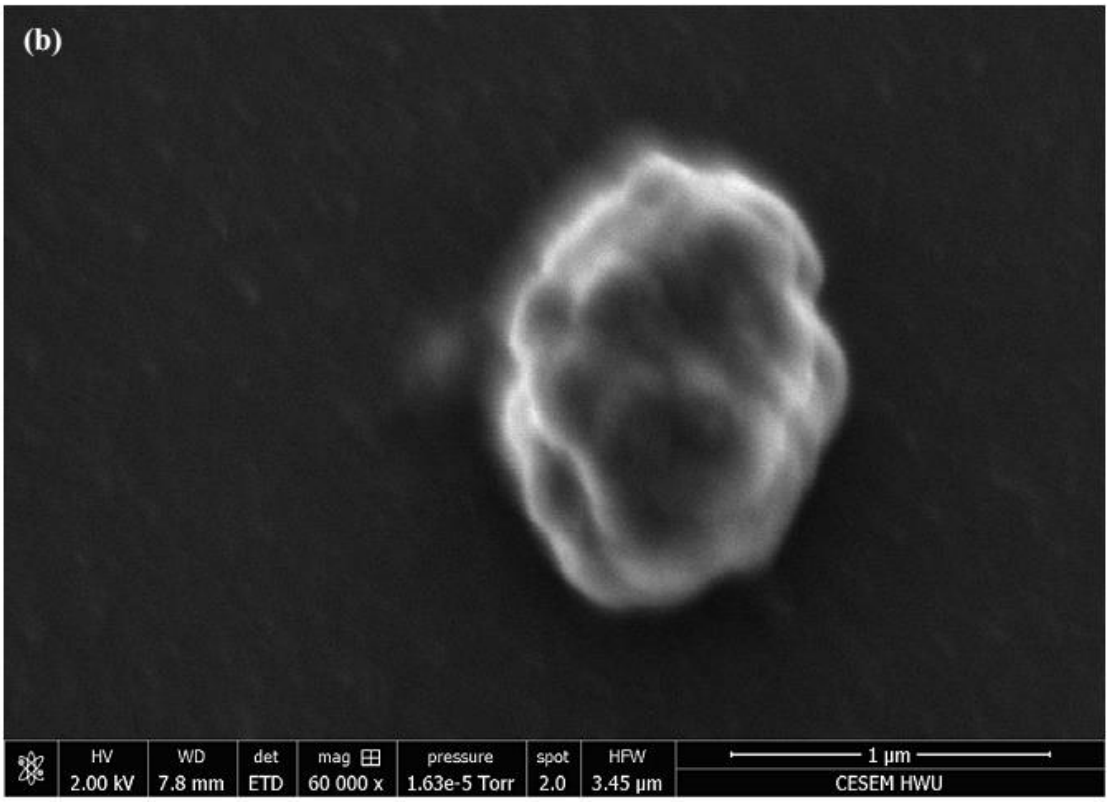

785

786 **Figure 6**

787

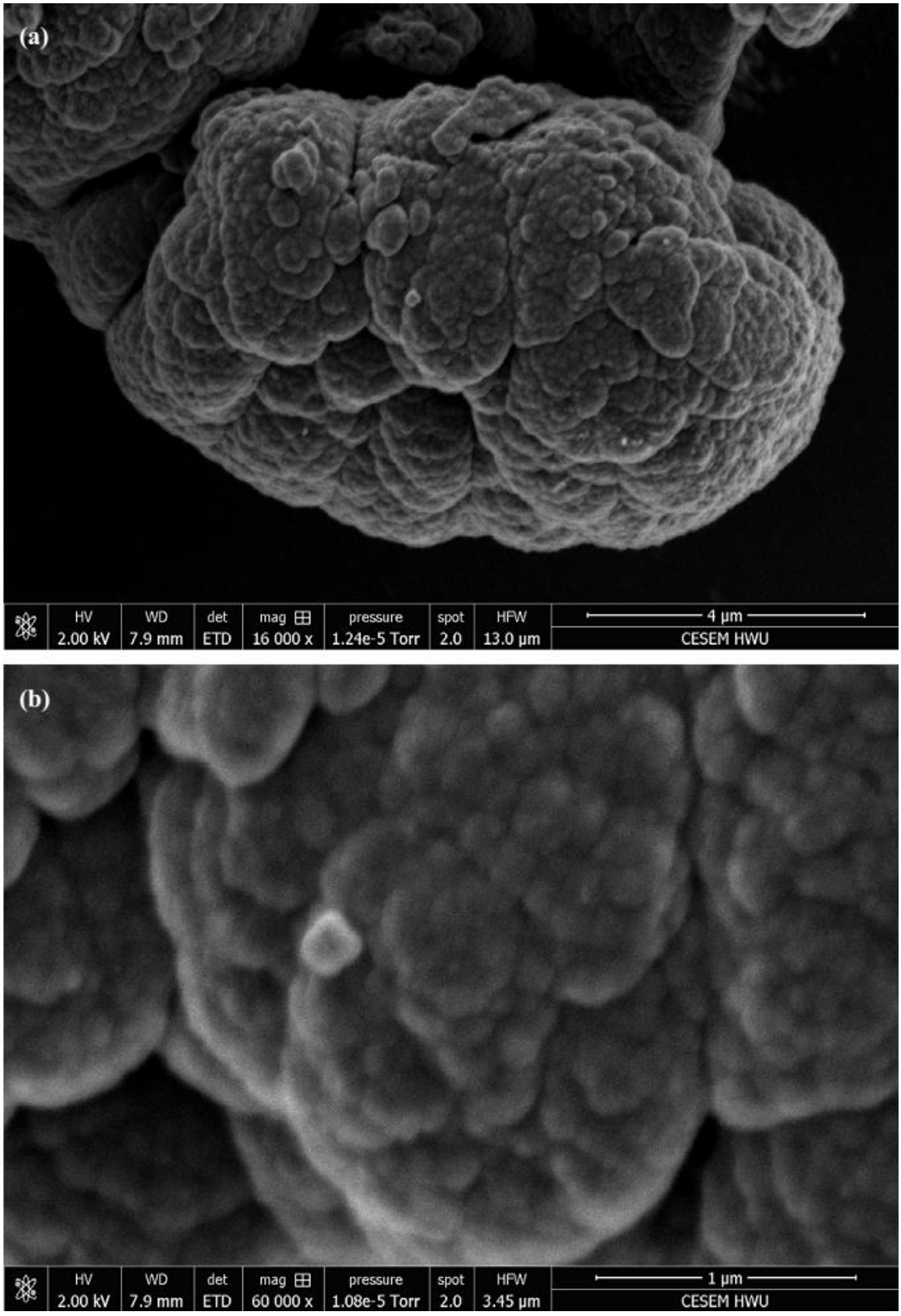
(a)
HV
2.00 kV
WD
7.9 mm
det
ETD
mag
16 000 x
pressure
1.24e-5 Torr
spot
2.0
HFW
13.0 µm
4 µm
CESEM HWU
(b)
HV
2.00 kV
WD
7.9 mm
det
ETD
mag
60 000 x
pressure
1.08e-5 Torr
spot
2.0
HFW
3.45 µm
1 µm
CESEM HWU

Figure 7

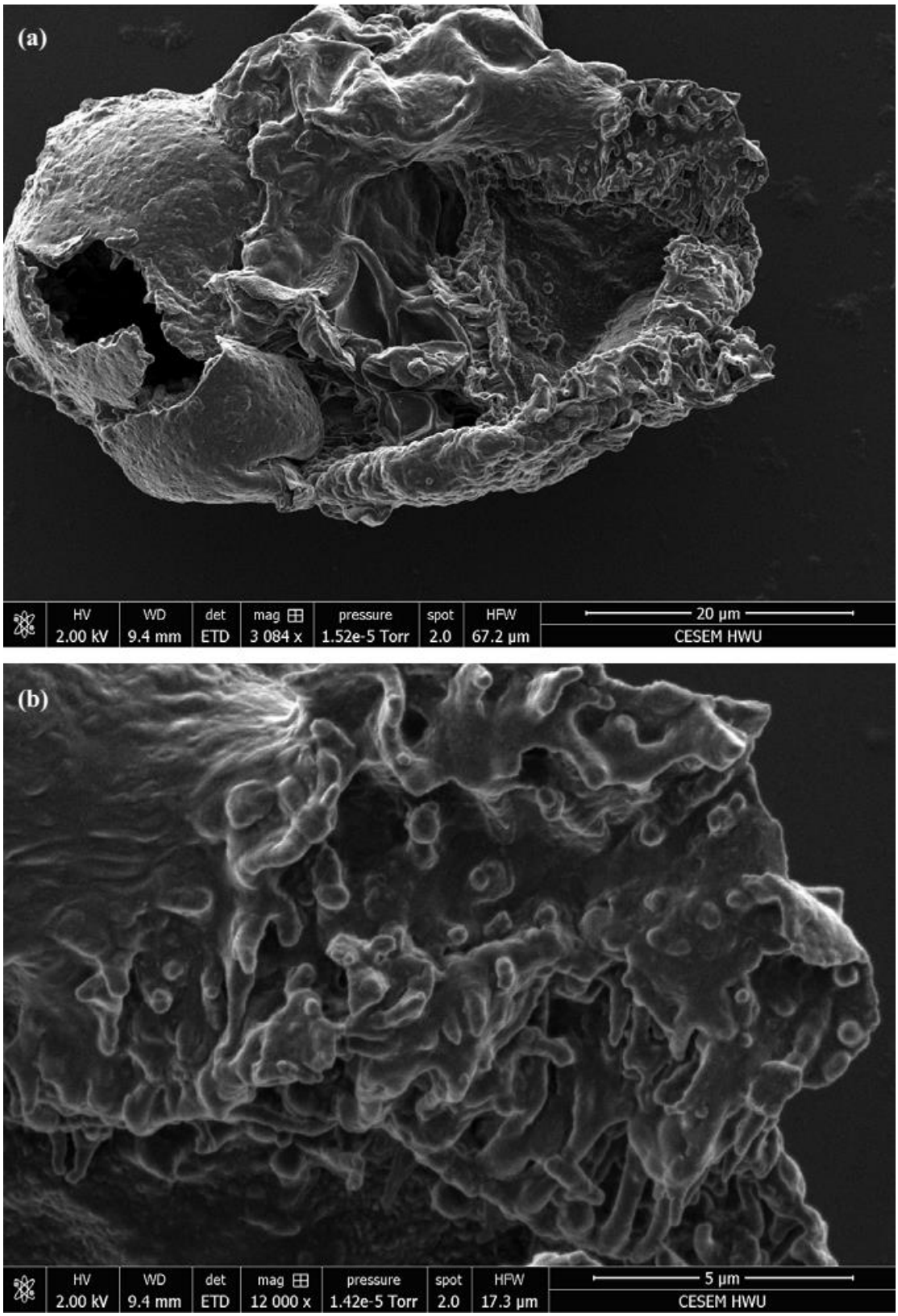
(a)
HV
2.00 kV
WD
9.4 mm
det
ETD
mag
3 084 x
pressure
1.52e-5 Torr
spot
2.0
HFW
67.2 µm
20 µm
CESEM HWU
(b)
HV
2.00 kV
WD
9.4 mm
det
ETD
mag
12 000 x
pressure
1.42e-5 Torr
spot
2.0
HFW
17.3 µm
5 µm
CESEM HWU

Figure 8

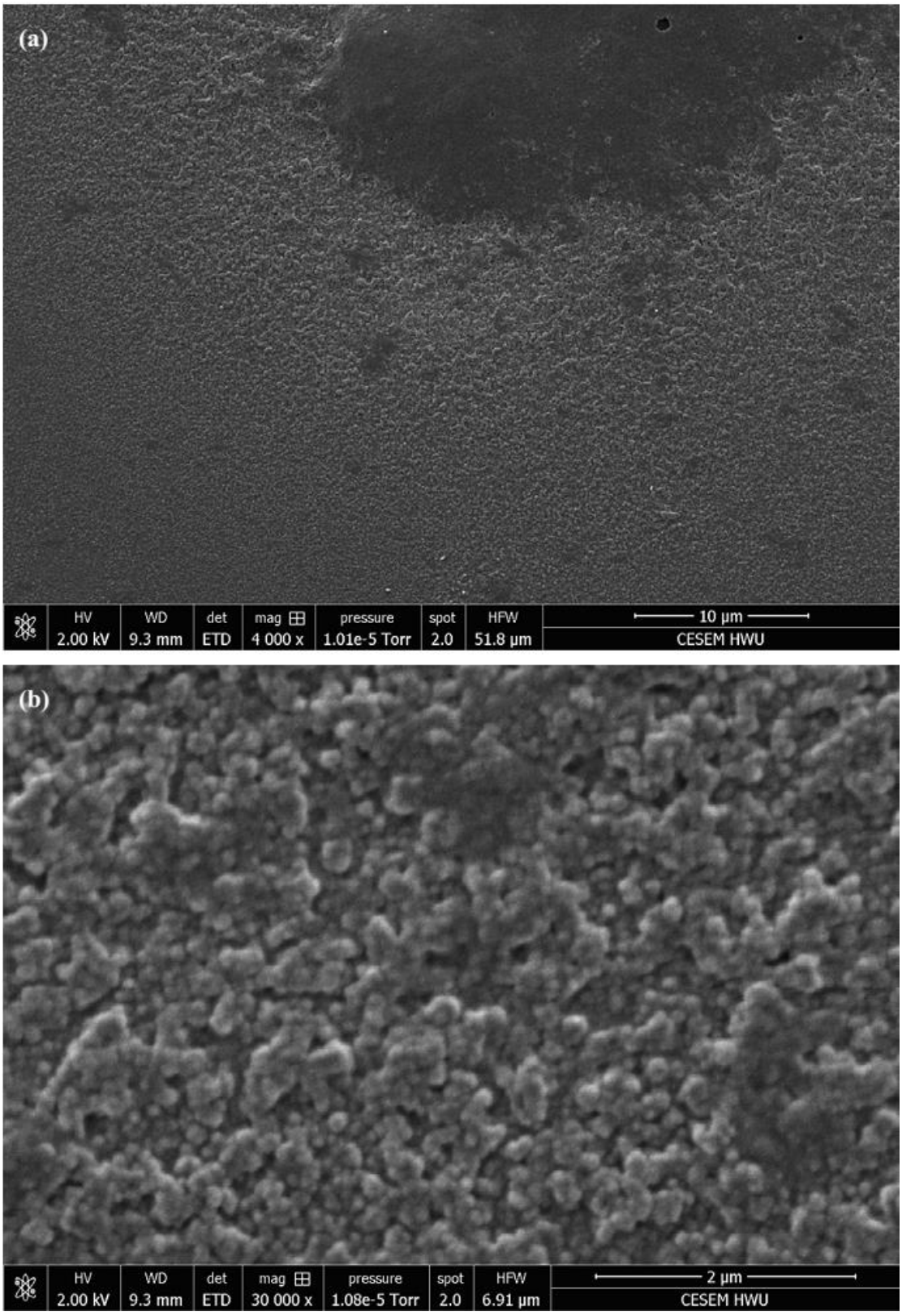
(a)
HV
2.00 kV
WD
9.3 mm
det
ETD
mag
4 000 x
pressure
1.01e-5 Torr
spot
2.0
HFW
51.8 µm
10 µm
CESEM HWU
(b)
HV
2.00 kV
WD
9.3 mm
det
ETD
mag
30 000 x
pressure
1.08e-5 Torr
spot
2.0
HFW
6.91 µm
2 µm
CESEM HWU

Figure 9

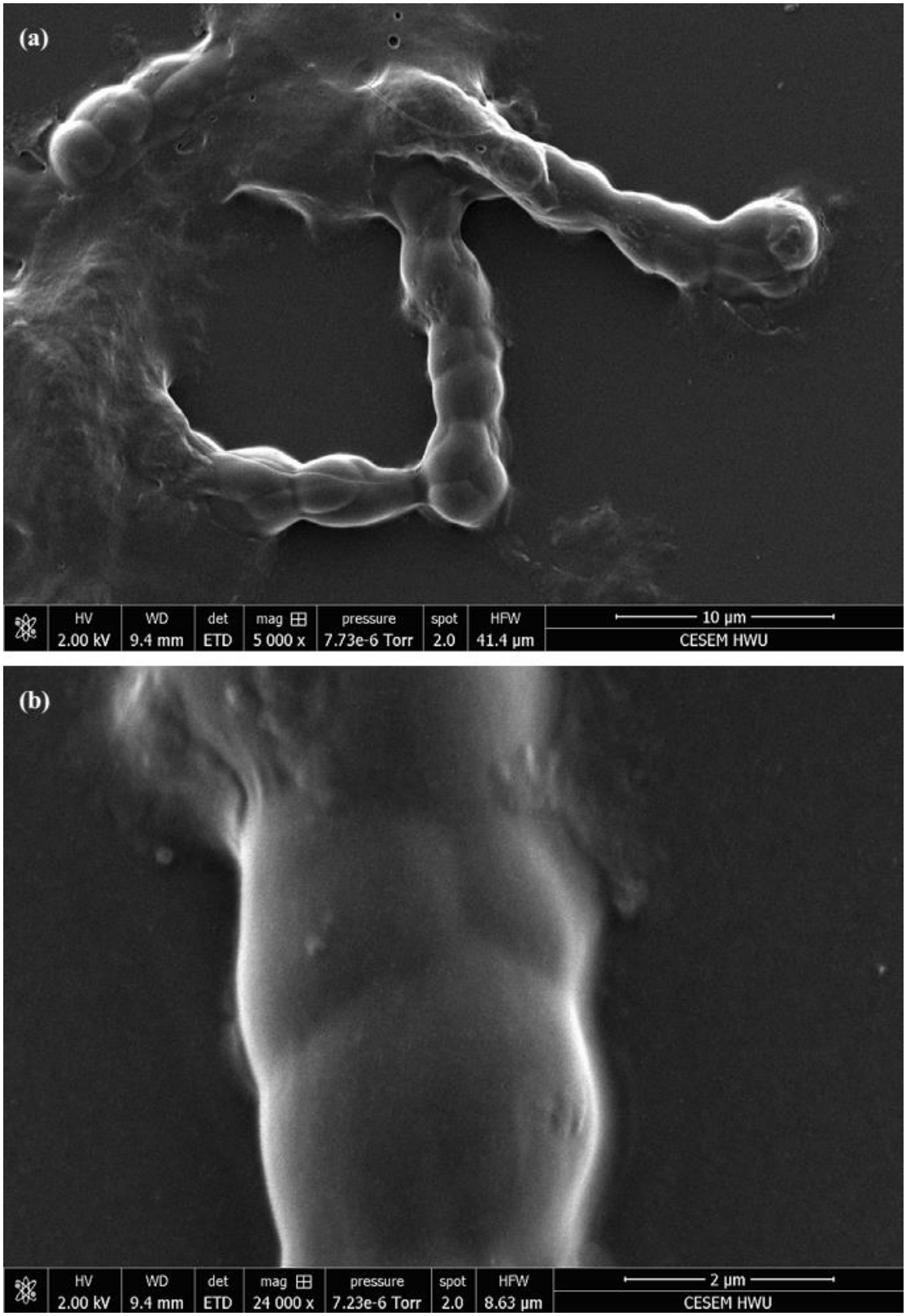
(a)
HV
2.00 kV
WD
9.4 mm
det
ETD
mag
5 000 x
pressure
7.73e-6 Torr
spot
2.0
HFW
41.4 µm
10 µm
CESEM HWU
(b)
HV
2.00 kV
WD
9.4 mm
det
ETD
mag
24 000 x
pressure
7.23e-6 Torr
spot
2.0
HFW
8.63 µm
2 µm
CESEM HWU

Figure 10

804

805

806

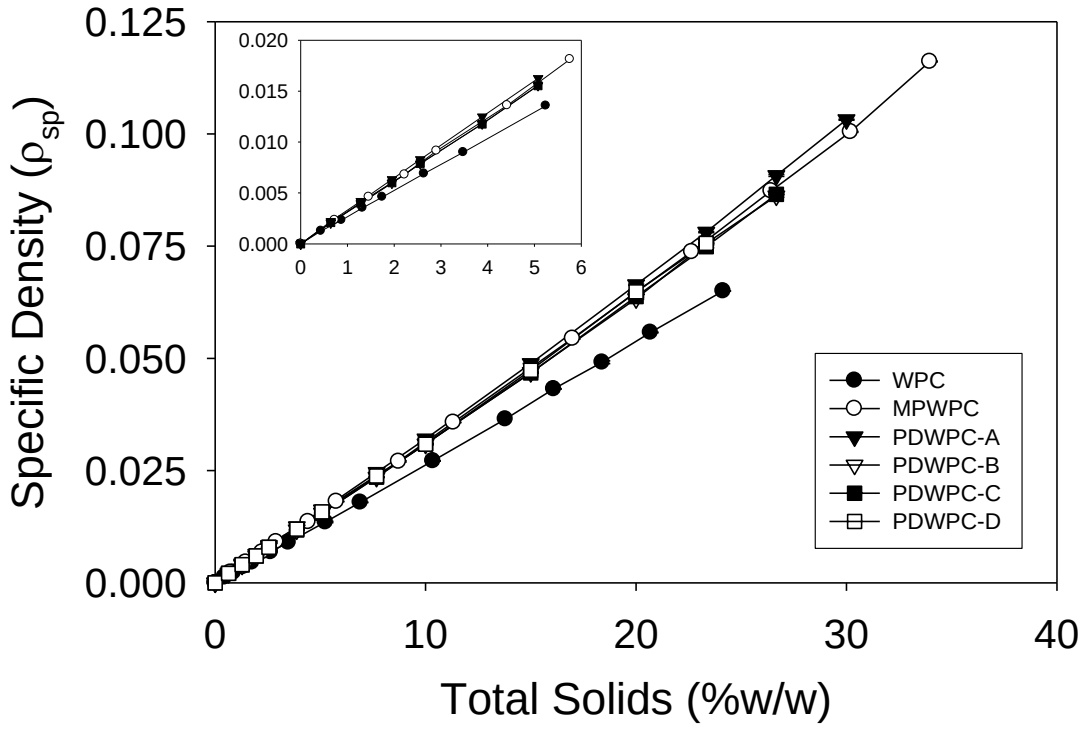

807

808

809 **Figure 11**

810

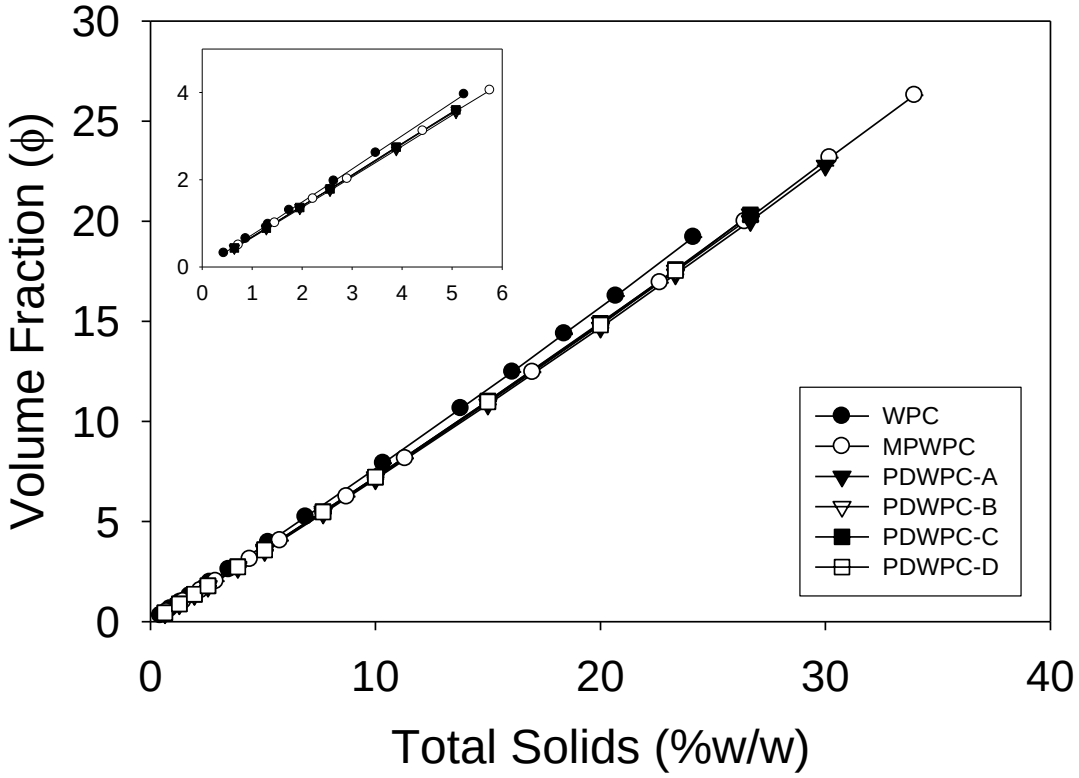
Volume Fraction (ϕ)
Total Solids (%w/w)
0
5
10
15
20
25
30
0
10
20
30
40
0
2
4
0
1
2
3
4
5
6
WPC
MPWPC
PDWPC-A
PDWPC-B
PDWPC-C
PDWPC-D

Figure 12

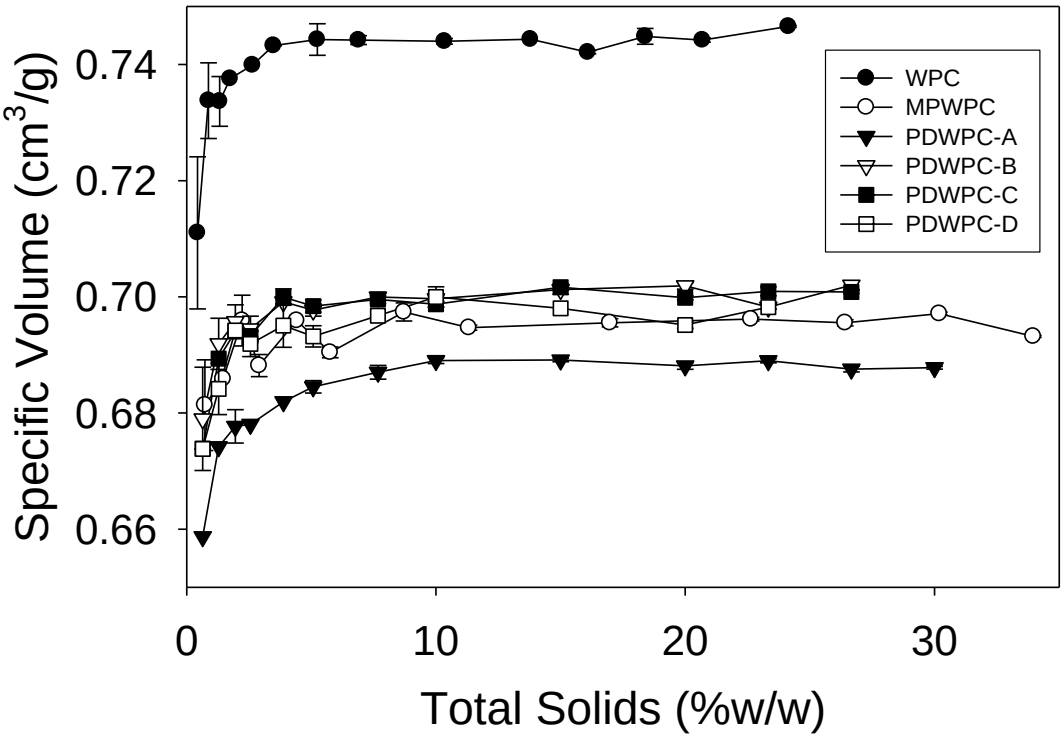
Specific Volume (cm3/g)
0.74
0.72
0.70
0.68
0.66
0
10
20
30
Total Solids (%w/w)
WPC
MPWPC
PDWPC-A
PDWPC-B
PDWPC-C
PDWPC-D

Figure 13